

13

Abstract

14 The Mojave Desert presents an array of Pleistocene lacustrine deposits and aeolian landforms to
15 which, at times, it has proved challenging to apply luminescence methods. We tested the suitability
16 of K-feldspar post-IR IRSL methods using two sites with independent radiocarbon dating – shorelines
17 at Harper Lake and Silver Lake – considering: 1) overall performance of the post-IR IRSL 225°C
18 (pIRIR₂₂₅) protocol, 2) effect of test dose size on pIRIR₂₂₅ D_e, 3) anomalous fading correction of
19 pIRIR₂₂₅ ages; 4) preliminary single grain pIRIR₂₂₅ results.

20 We observe consistently good performance of the single aliquot pIRIR₂₂₅ protocol, with good dose
21 recovery, acceptable recycling ratios, low recuperation and low inter-aliquot scatter. The pIRIR₂₂₅
22 ages for Silver Lake (8.8 ± 0.4 and 11.3 ± 0.5 ka) and Harper Lake (both 25.4 ± 1.4 ka) are in
23 substantially better agreement with the independent dating than low temperature (50°C) IRSL and
24 quartz OSL ages. pIRIR₂₂₅ fading rates are reduced to ~2.0-2.5% per decade, but there remains a
25 tendency for under-estimation when using uncorrected ages. A need for fading correction is further
26 implied at Harper Lake via comparison with multi-elevated temperature (MET)-PIR age plateaus and
27 pIRIR₂₉₀ measurements, although at the younger Silver lake site these methods produce ages nearly
28 identical to the uncorrected pIRIR₂₂₅ ages. Preliminary single grain pIRIR₂₂₅ measurements suggest a
29 ~25-30% usable grain yield. At Silver Lake the single grain and single aliquot ages agree well despite
30 over-dispersion of the single grain equivalent dose distribution. At Harper Lake the single grain and
31 single aliquot pIRIR₂₂₅ ages also agree well, although a population of insensitive, lower D_e grains is
32 observed. These grains are not associated with significantly higher fading rates.

33

34

35

36 Introduction

37 The Mojave Desert (southwest USA) preserves abundant evidence for Pleistocene palaeo-lakes
38 (Enzel et al., 2003) and relict aeolian deposits (Lancaster and Tchakerian, 1996). Various
39 luminescence dating methods have been applied, including quartz optically stimulated luminescence
40 (OSL) (Bateman et al., 2012; Fuchs et al., 2015), K-feldspar thermoluminescence (TL) and infra-red
41 stimulated luminescence (IRSL; Clarke et al. 1995; Rendell and Sheffer, 1996). Presently there are
42 conflicting ages between studies (e.g. Rendell and Sheffer, 1996 and Bateman et al., 2012), within
43 sites (stratigraphic inversions), and contrasting results compared to independent dating (e.g. Owen
44 et al., 2007). Quartz may be an unreliable dosimeter in the Mojave due to its low sensitivity and a
45 contaminating K-feldspar signal (Lawson et al., 2012). K-feldspar is, however abundant in Mojave
46 sediments and is a potentially advantageous mineral choice given the relatively high environmental
47 dose rates (typically $> 3 \text{ Gy ka}^{-1}$). Previous applications of K-feldspar IRSL (Rendell and Sheffer, 1996)
48 did not include anomalous fading correction and subsequent studies using low temperature IRSL
49 have reported variable, but sometimes high fading rates (Garcia et al., 2014).

50 We consider the reliability of K-feldspar ages derived via post-IR IRSL (pIRIR) methods, which
51 can isolate a slower (or non) fading IRSL signal (Thomsen et al., 2008; Buylaert et al., 2012).
52 Demonstrating the suitability of pIRIR approaches would be an important step in improving
53 chronological control in the Mojave, and recent applications have shown promise (McGuire and
54 Rhodes, 2015; Roder et al., 2012). We sampled two sites with independent dating to consider pIRIR
55 protocol performance.

56 Study sites

57 Two palaeo-lakes in the Mojave River catchment were analysed; Harper Lake and Silver Lake (**Figure**
58 **1**). Sourced in the San Bernardino Mountains to the southwest, the Mojave River experienced
59 episodes of perennial flow during the Pleistocene, periodically maintaining Lake Manix, Harper Lake
60 and the downstream Silver Lake. This catchment history is discussed elsewhere (Meek, 1999; Enzel
61 et al., 2003; Wells et al., 2003; Reheis et al., 2012; 2015).

62 Silver Lake formed part of pluvial Lake Mojave (Wells et al., 2003) (**Figure 1a; 1c**). Several
63 sites demonstrate lake high-stands (following Wells et al., 2003) at ~22-19 cal ka BP (18.4-16.6 ka;
64 “Lake Mojave 1”) and ~16.6-13.3 cal ka BP (13.7-11.4 ka; “Lake Mojave 2”), with intermittent
65 inundation at 13.3-9.8 cal ka BP (~11.4-8.7 ka). A spit-shoreline complex at “Silver Quarry” (Ore and
66 Warren, 1978) was subject to a detailed investigation combining radiocarbon dating of the
67 freshwater bivalve *Anodonta californiensis*, quartz OSL and fine-grain K-feldspar IRSL Multi-Aliquot
68 Additive Dose (MAAD) methods (Owen et al., 2007). Our luminescence samples were obtained from
69 Owen et al.’s (2007) LithoFacies Associations (LFA) LFA8 (SL14-1; 0.4 m) and LFA6 (SL14-2; 1.2 m)
70 (**Figure 1c**). Using the BCal Bayesian analysis software (**Table S2**), Owen et al. (2007) assigned age
71 ranges of 12.1-11.6 cal ka BP to LFA 8 (7 dates) and 12.2-12.5 cal ka BP to LFA 6 (2 dates). Their
72 quartz OSL ages for LFA 8 (SL125) and LFA6 (SL126) were 6.6 ± 0.7 ka and 6.5 ± 0.6 ka respectively.

73 Harper Basin (**Figure 1a**) is presently isolated from the Mojave River, but was likely fed by
74 periodic Mojave River avulsions (Meek, 1999). Lake beds are exposed at ‘Mountain View Hill’ where
75 radiocarbon dates from *A. californiensis* shells of 24,055-33,059 cal yr. BP ($24,440 \pm 2190$ ^{14}C yr BP)
76 and 28,375-29,790 cal yr. BP ($25,000 \pm 310$ ^{14}C yr. BP) were first reported (with a third infinite age;
77 Meek, 1999). Garcia et al. (2014) presented eight new *A. californiensis* radiocarbon dates and
78 luminescence ages from coarse-grain (125-150 μm) post-IR quartz SAR and fine grain (4-11 μm) K-
79 feldspar MAAD IRSL (**Figure 1b**). The new radiocarbon dates ranged from 33,410 to 39,788, cal yr.
80 BP; **Table S2; Figure 1b**), with fading-corrected IRSL ages of 28 ± 2 ka to 46 ± 3 ka (7.2% per decade
81 fading rate). The quartz ages were substantially younger (17-19 ka). Garcia et al. (2014) argued for a
82 probable age of 40-45 ka, but there is variability within and between the radiocarbon and IRSL ages,
83 with the former close to the limits of the method. The independent dating control at Harper Lake is
84 thus less firm than Silver Lake. We sampled the same section and took samples from the beach unit
85 (figure 5 of Garcia et al., 2014) at 0.84 and 1.25 m (**Figure 1c**).

86 Methods

87 180-250 μm quartz and K-feldspar grains were isolated, with K-rich feldspars obtained via density
88 separation at 2.58 g cm^{-3} and etched in 10% HF for 10 minutes. All samples were analysed on a Risoe
89 DA20 TL/OSL reader, with quartz luminescence detected through a Hoya U340 filter and IRSL
90 through Schott BG39 and Corning 7-59 filters. Quartz equivalent doses on 2 mm aliquots were
91 determined using the single aliquot regeneration (SAR) protocol (Murray and Wintle, 2000)
92 employing post-IR (50°C) blue LED (125°C) stimulation. 2 mm aliquots of K-feldspar were analysed
93 using a pIRIR protocol comprising a 50°C IRSL stimulation and a subsequent 225°C stimulation
94 (henceforth pIRIR₂₂₅) with a 250°C preheat (1 minute). Anomalous fading rates were determined
95 following Auclair et al. (2003) with corrections following Huntley and Lamothe (2001), using the R
96 package "Luminescence" (Kreutzer et al., 2012).

97 Dose rates were determined using *in-situ* gamma spectrometry and ICP-MS (**Table S1**). We
98 used the estimated water contents of Owen et al. (2007) and Garcia et al. (2014) ($10 \pm 5 \%$ and 14.5
99 $\pm 5\%$ respectively). A 5 % absolute change in water content produces an age difference of 200-300
100 years at Silver Lake and ~ 380 years at Harper Lake.

101

102 Results

103 Silver Lake

104 pIRIR₂₂₅ ages (**Table 1 and Figure S1**) were obtained using a moderate (23% of D_e) test dose. Sample
105 SL14-1 (LFA8) produced a fading-uncorrected pIRIR₂₂₅ age of $8.8 \pm 0.4 \text{ ka}$, and sample SL14-2 (LFA6)
106 an age of $11.3 \pm 0.5 \text{ ka}$. The pIRIR₂₂₅ residual D_e s following 48 hours of (UK) daylight were 0.8 and 1.0
107 Gy. A quartz OSL age of $5.2 \pm 0.5 \text{ ka}$ for SL14-1 (LFA8) is comparable to that of Owen et al. (2007) and
108 is much younger than the radiocarbon dates. All quartz aliquots are rejected if the fast ratio criterion
109 (average ratio 2.4 ± 1.7) is applied (Durcan and Duller, 2011) and in light of the signal contamination

110 test results (**Figure S2**, after Lawson et al. 2012;) this age is considered unreliable. We infer this
111 probably also applies to Owen et al.'s (2007) quartz ages.

112 The pIRIR₂₂₅ ages are in better agreement with the radiocarbon dating (BCal ages 12.1-11.6
113 cal yr. BP and 12.5-12.2 cal. yr BP for LFA8 and LFA6). They show low D_e over-dispersion (3-6%;
114 **Figure S1**), good dose recovery (ratios 1.00 ± 0.01 (SL14-1) and 0.99 ± 0.01 (SL14-2)), low
115 recuperation (<2 % for all aliquots) and recycling ratios consistent with unity (e.g. SL14-1 average
116 1.02 ± 0.02). The SL14-1 fading-uncorrected pIRIR₂₂₅ age is younger than the LFA8 BCal radiocarbon
117 age range, although it is within uncertainties of the youngest radiocarbon date from this LFA (AP9;
118 9081-9322 cal. yr BP; **Table S2; Figure S4**). SL14-2 is within 2 sigma uncertainties of the LFA6 BCal
119 age (12.2-12.5 ka). Thus, although both pIRIR₂₂₅ ages show better agreement with the independent
120 dating, it is prudent to consider possible underestimation relative to the radiocarbon dating.

121

122 *Test dose size*

123 Test dose size has been shown to impact sample D_e within pIRIR protocols (Li et al., 2014; Lui et al.,
124 2016; Yi et al., 2016; Colarossi et al., 2018). At Silver Lake the natural D_e was determined for test
125 doses between 4 and 65% of the expected D_e (**Figure 2**). The results suggest possible age
126 underestimation at low test doses (but note the uncertainties), with a much clearer tendency at high
127 doses. Moderate (23-30% of D_e) test doses produced ages closest the expected age. Considering the
128 dose response curves (DRC) for low (3.8%), moderate (27% of D_e) and high (65% of D_e) test doses
129 (**Figure S3**), low test dose DRCs saturate faster (D₀ = ~43 Gy compared to > 150 Gy for 27% test dose),
130 with little difference between moderate and high test doses. The age difference between moderate
131 and high test doses seems to reflect a lower Ln/Tn for the latter. The test dose used for the age
132 estimates in **Table 1** (23%) is thus unlikely to be a source of age-underestimation.

133

134 *Ages and fading rates*

135 The pIRIR₂₂₅ fading rates are $2.1 \pm 0.3\%$ and $0.7 \pm 0.3\%$ per decade for SL14-1 and SL14-2 and fading
136 correction brings them into better (SL14-1) and very good (SL14-2) agreement with the radiocarbon
137 ages (**Table 1; Figure S4**). The fading rates for the IR 50°C are $6.5 \pm 0.3\%$ and $5.6 \pm 0.4\%$ for SL14-1
138 and SL14-2, but with fading-correction (10.3 ± 0.6 and 12.4 ± 0.8 ka) they show good
139 correspondence with the fading-corrected pIRIR₂₂₅ and radiocarbon ages.

140 The need for fading correction of the post-IR IRSL signal may be removed by using a
141 higher temperature second IR stimulation (pIRIR₂₉₀; Buylaert et al., 2012). This is usually at the
142 expense of a larger unbleached/residual IRSL signal (Kars et al., 2014) and in water-lain deposits, it
143 may be advantageous to utilise a more easily bleached signal (i.e. pIRIR₂₂₅). To assess this further, we
144 compared the pIRIR₂₂₅ ages and independent ages with the pIRIR₂₉₀ (Buylaert et al., 2012) and
145 multiple elevated temperature (MET) PIR (Li and Li, 2011) methods. For sample SL14-1, we observe
146 possible MET-PIR plateau above 200°C, but the 250°C age (8.8 ± 0.5 ka) matches the fading-
147 uncorrected pIRIR₂₂₅ age (**Figure 3**). Although pIRIR₂₉₀ and MET-300°C data are broadly within this
148 range, they show more inter-aliquot scatter, perhaps indicating the unsuitability of higher
149 preheating/stimulation temperatures. Increasing the first stimulation temperature (for pIRIR₂₂₅) to
150 80°C or 110°C increases the age of SL14-1 to 9.9 ± 0.4 and 9.7 ± 0.4 ka, perhaps implying removal of
151 a fading-prone signal. However, the trend does not continue with higher (180°C) first stimulation
152 temperatures (8.7 ± 0.5 ka). Thus, the MET-PIR 250°C age, pIRIR₂₉₀ and the uncorrected pIRIR₂₂₅ age
153 for SL14-1 all fall at the lower edge of the expected BCal age range (**Figures 3 and S4**) and it is
154 presently unclear whether the MET plateau represents a non-faded age.

155 *Single grain analysis*

156 The single aliquot data show limited inter-aliquot scatter, but given potential signal averaging for K-
157 feldspars (Trauerstein et al. 2014) and the lacustrine context, preliminary single grain measurements
158 were conducted for SL14-1. Grains were mounted on single aliquot disks and stimulated with the IR
159 LED. A dose recovery experiment was conducted, comprising room temperature IR bleaching for 200

160 seconds and a 33 Gy dose. Of 96 analysed, 22 grains produced acceptable signals (test dose > 3
161 sigma above background, recycling ratios between 0.8 and 1.2, recuperation < 5%). The central age
162 model (CAM) dose recovery ratio was 1.02 ± 0.03 (identical to arithmetic mean). The D_e over-
163 dispersion from the dose recovery experiment was low at $3.3 \pm 0.4\%$ (cf. Rhodes, 2015; Brown et al.,
164 2015). This OD was added to the individual grain D_e uncertainties for analysis of the natural D_e . A
165 natural equivalent dose was derived from 21 grains (of 96 measured). The data show significant (37
166 $\pm 6\%$) over-dispersion, but the CAM-derived age (8.9 ± 0.9 ka) is identical to the single aliquot result
167 (**Figure 4**). The distribution of grain brightness (**Figures 4 and S5**) is skewed (50% of light sum from
168 18% of grains), but there is no relationship between grain sensitivity and equivalent dose (c.f.
169 Rhodes, 2015), nor is there a correlation between grain fading rates and equivalent dose.

170 Harper Lake

171 Harper Lake produced two identical pIRIR₂₂₅ ages (test dose 10% of D_e) of 25.4 ± 1.4 ka (**Table 1**;
172 **Figure S1**). The fading-uncorrected ages are within uncertainties of one of Meek's (1999)
173 radiocarbon ages, lower than all other radiocarbon ages, and within uncertainties of one fine-grain
174 IRSL age (28 ± 2 ka) (Garcia et al., 2014; **Figure S6**). pIRIR₂₂₅ data show good dose recovery ($0.98 \pm$
175 0.01 (HL14-1) and 0.97 ± 0.01 (HL14-2)), good recycling ratios (averages 1.01 ± 0.02 and 1.02 ± 0.02)
176 and low recuperation (all aliquots < 0.5%). Residuals following 48 hours of daylight were 5.5 and 3.5
177 Gy. The 50°C IR ages are 13.0 ± 0.7 ka and 13.9 ± 0.8 ka. Quartz performance was poor (**Figures S2**
178 **and S6**) with most aliquots rejected for excessive recuperation (average ~13%) using late
179 background subtraction. A quartz age for HL14-1 from 3 acceptable aliquots using early background
180 subtraction was 25.7 ± 4.4 ka, and 23.6 ± 2.8 ka for the single acceptable aliquot using late
181 background subtraction.

182 Test dose size

183 For Harper Lake, the effect of test dose size was investigated with a dose recovery experiment and
184 using the natural IRSL D_e (**Figure 2**). The natural measurements show little sensitivity to test dose
185 size, but the lowest test dose (2.5%) produced significant inter-aliquot scatter. The dose recovery

186 experiment suggests underestimation at test doses >30% of D_e , with a relatively low test dose (8%)
187 giving the best dose recovery (0.98 ± 0.01 ; $n=3$). For both the natural and dose recovery
188 measurements, the DRCs behave as per Silver Lake, with faster saturation for the lowest test doses
189 (D_0 of 100 ± 3 Gy for the 2.5% test dose vs. 306 ± 52 Gy for 48% test dose) and indistinguishable
190 DRCs for moderate (23%) and high (65%) test doses (**Figure S3**). Despite this, lower test doses
191 produced the best dose recovery, with a tendency for lower \ln/T_n ratios rather than a changing DRC
192 at high test doses. The latter was not observed in the natural D_e measurements.

193 *Fading rates*

194 The 50°C IR fading rates are 10.6 ± 2.0 % and 9.4 ± 1.0 % per decade for HL14-1 and 14-2, resulting in
195 large uncertainties with fading-correction. The pIRIR₂₂₅ fading rates are comparable to Silver Lake
196 (2.0 ± 0.4 and 2.4 ± 0.2 %), but the MET-PIR plateau for HL14-2 more unambiguously implies a need
197 for fading correction (**Figure 3**), with the 250°C age of 35.4 ± 2.5 ka within uncertainties of several of
198 Garcia et al.'s (2014) radiocarbon ages (**Figure S6**). The pIRIR₂₉₀ ages are comparable to this ($33.4 \pm$
199 1.9 ka and 37.3 ± 2.3 ka for HL14-1 and HL14-2 respectively; **Figures 3 and S6**), although the pIRIR₂₉₀
200 dose recovery results for HL14-1 (1.07 ± 0.05 $n=2$) (natural dose plus a 66.5 Gy dose) hint at
201 potential overestimation. The fading-corrected pIRIR₂₂₅ ages for both HL14-1 and HL14-2 are $29.0 \pm$
202 1.9 ka and 29.8 ± 2.0 ka, placing them good agreement with Meek's (1999) radiocarbon ages, but
203 still somewhat lower than Garcia et al.'s (2014) radiocarbon ages (**Figure S6**) and most of their IRSL
204 ages.

205 *Single grain analysis*

206 28 of 96 grains from HL14-1 produced acceptable luminescence characteristics. The distribution of
207 grain brightness (**Figure S5**) is skewed (~20% of grains account for 50% of the light sum) and the
208 equivalent dose distribution is over-dispersed (29 ± 4 %, with 3.3% added to individual uncertainties).
209 A cluster of lower D_e grains are also insensitive (**Figure 4**), but are not associated with higher fading
210 rates (**Figure S7**). The CAM D_e using all grains is 94.0 ± 6.2 Gy, but increases to 112.4 ± 6.1 Gy when

211 the brightest 50% are used ($n=14$), and the D_e distribution becomes less dispersed ($OD 16 \pm 4\%$). The
212 (fading uncorrected) age using the brightest grains (26.8 ± 1.9 ka) is indistinguishable from the single
213 aliquot age. Individual grain fading rates range from 11% to -6% per decade. Although the
214 uncertainties are large, the mean is comparable to the single aliquot analysis (2.8 % per decade).

215 Discussion

216 Comparison with independent dating is limited by several factors. For Harper Lake there are
217 inconsistencies between the radiocarbon chronologies of Meek (1999) and Garcia et al. (2014).
218 Garcia et al.'s (2014) preferred site age was older still at 40-45 ka (citing palaeosol ages in the down-
219 catchment Lake Manix Basin (Reheis et al., 2012) and noting that post-depositional contamination
220 would tend to make radiocarbon ages too young; see also Reheis et al., 2015). However, the precise
221 reasons remain unclear, and the spread of ages makes interpretation difficult (Reheis et al., 2015).
222 The impact of the hard-water effect on radiocarbon ages was suggested by Owen et al. (2007) to be
223 < 150 years, although Berger and Meek (1992) reported offsets up to 450 years. For luminescence
224 ages there are also potential offsets from water content estimation. Using water contents at
225 saturation ($\sim 35\%$) or akin to the modern values (2 %) results in $pIRIR_{225}$ ages of 8.5-9.6 ka for SL14-
226 1/LFA8 and 23.8-27.8 ka for HL14-1. Given these are extreme values, it is unlikely that this alone
227 accounts for any differences (for Harper Lake particularly).

228 Nonetheless, the $pIRIR_{225}$ ages show substantially better agreement with the independent
229 dating than the 50°C IR and quartz OSL ages (**Table 1; Figures S4 and S6**). The single aliquot $pIRIR_{225}$
230 data are highly reproducible and an absence of overestimation at either site implies incomplete
231 bleaching is not an issue, despite the lacustrine contexts. Lower 50°C IR ages reflect a need for
232 anomalous fading correction (noting the inter-site variability) (**Table 1**), while quartz
233 underestimation reflects low sensitivity and (probably) a significant contaminating non-quartz signal
234 (**Figure S2**). At Harper Lake a small proportion of quartz aliquots produce ages in better agreement
235 with the $pIRIR_{225}$ ages with early background signal subtraction or if the fast ratio (Durcan and Duller,

236 2011) is employed as screening methods (Hay, 2018). The aliquot rejection rate is high and the ages
237 are still lower than the fading-corrected pIRIR₂₂₅ ages, and much of the independent chronology.
238 Quartz ages not employing such rigorous screening (at least, quartz of local origin) should be
239 considered with care.

240 Limited sensitivity of the natural D_e to test dose size is observed for test doses between 5
241 and ~56% of D_e at Harper Lake and between 5 and 30% at Silver Lake. There is a clear impact on the
242 DRC for very small test doses (**Figure S3**), but this does not result in consistently higher or lower D_e
243 estimates (note the scatter for the low test doses for the Harper Lake natural signal; Lui et al., 2016).
244 At Harper Lake the dose recovery data appear more sensitive to test dose than the natural D_e data
245 (Yi et al., 2016). There is a significant correlation between Lx background and the Tx initial signals for
246 all test dose analyses (Colarossi et al., 2018), and the slope of this relationship increases at higher
247 test doses. There is a tendency towards poorer dose recovery at high test doses at Harper Lake. This
248 is due to a lower Ln/Tn (**Figure S3**), which is also seen in natural D_e data at Silver Lake. The reason(s)
249 for this is(are) not clear, but it implies an effect on the initial natural dose/test dose measurement.

250 At Silver Lake the fading-uncorrected pIRIR₂₂₅ ages are close(SL14-2) or fall below (14-1) the
251 radiocarbon age ranges. For SL14-1 especially this implies fading correction (2.1% per decade) is
252 necessary (**Table 1**). The MET-PIR data do not unambiguously support this however, although a small
253 increase in the first stimulation temperature does increase the sample age. At Harper Lake most
254 results from the independent dating and the MET-PIR / pIRIR₂₉₀ data more strongly indicate that
255 fading correction of the pIRIR₂₂₅ ages (2.0-2.4% per decade) is required. The MET-PIR plateau (200-
256 250°C) and pIRIR₂₉₀ data fall within the lower range of Garcia et al.'s (2014) radiocarbon dates. The
257 fine-grain MAAD IRSL ages (*ibid*) show less consistency than our coarse-grain pIRIR₂₂₅ and pIRIR₂₉₀
258 ages (samples ALG-HL-OSL2 vs ALG-HL-OSL3 in Garcia et al., 2014), which perhaps reflects
259 uncertainty imparted when correcting the former for the high 50°C IR fading rates at this site (**Table**
260 **1**), which was also based on fading analysis of a single sample.

261 The preliminary single grain data indicate (from dose recovery data) rather low “intrinsic”
262 over-dispersion (using the IR LED), but this requires further investigation (c.f. Rhodes, 2015). The
263 limited number of grains should be kept in mind. There is variability in both the signal contribution
264 from individual grains (**Figure S5**) and in the presence of a “declining baseline” (i.e. systematically
265 lower D_e s for the dimmest grains; Rhodes, 2015; **Figure 4**; **Figure S7**). At Harper Lake using the
266 brightest grains reduces OD and moves the resulting age closer to the independent dating (Lamothe
267 et al., 2012), but the result is still within uncertainties of the age obtained using all the grains. Such a
268 relationship is not seen at Silver Lake. At Harper Lake the insensitive, lower D_e grains do not have
269 higher fading rates (**Figure S7**). The internal K/Rb contents of the grains were not assessed, but some
270 studies suggest that K content may not be strongly associated with grain sensitivity (Smedley et al.,
271 2012) or fading rate (Trauerstein et al., 2014).

272 Conclusions

273 The pIRIR₂₂₅ protocol shows significantly better agreement with independent dating than the 50°C IR
274 and quartz OSL ages in the Mojave region studied. Quartz consistently and significantly
275 underestimates expected sample ages. At both sites the pIRIR₂₂₅ ages show improved agreement
276 with the independent dating after fading correction, with the MET-PIR and pIRIR₂₉₀ results showing
277 even better agreement with independent ¹⁴C ages (of Garcia et al., 2014) at Harper Lake. However,
278 this is not always the case, as at the younger Silver Lake site the SL14-1 MET-PIR and pIRIR₂₉₀ ages
279 are identical to the uncorrected pIRIR₂₂₅ age. The pIRIR₂₂₅ measurements show limited sensitivity to
280 test dose size at Harper Lake, but at both sites the DRCs saturate faster for low test doses and
281 underestimate for high test doses at Silver Lake. The latter is not observed at Harper Lake where the
282 dose recovery data seem to be more sensitive to test dose size than the natural D_e measurements.
283 Contrasting single grain behaviors are also observed, notably in the presence of less sensitive, lower
284 D_e grains at Harper Lake. This mirrors some previous work in suggesting, at least for some sites, that
285 the brightest K-feldspar grains may provide a better estimate of burial dose.

286 [Acknowledgments](#)

287 ASH was supported by NERC studentship 1358108. Rob Fulton, Jason Wallace and Simon Benson are
288 thanked for logistical support. An anonymous reviewer is thanked for very constructive comments.

289

290 [References](#)

291 Auclair, M., Lamothe, M. Huot, S. 2003. Measurement of anomalous fading for feldspar IRSL using
292 SAR. *Radiation Measurements* 37, 487-492.

293 Bateman, M.D., Bryant, R.G., Foster, I.D.L., Livingston, I. Parsons, A.J. 2012. On the formation of sand
294 ramps: A case study from the Mojave Desert. *Geomorphology* 161-162, 93-109.

295 Berger, R., Meek, N. 1992. Radiocarbon dating of *Anodonta* in the Mojave River basin. *Radiocarbon*,
296 34, 578-584.

297 Brown, N.D., Rhodes, E.J., Antinao, E.V., McDonald, E.V. 2015. Single grain post-IR IRSL signals of K
298 feldspar of alluvial fan deposits in Baja California Sur, Mexico. *Quaternary International* 362, 132-
299 138.

300 Buylaert, J-P., Jain, M., Murray, A.S., Thomsen, K.J., Theil, C. Sohbaty, R. 2012. A robust feldspar
301 luminescence dating method for Middle and Late Pleistocene sediments. *Boreas* 41, 435-451.

302 Colarossi, D., Duller, G.A.T., Roberts, H.M. 2018. Exploring the behaviour of luminescence signals
303 from feldspars: Implications for the single aliquot regenerative dose protocol. *Radiation*
304 *Measurements*. 109, 34-44.

305 Clarke, M.L., Richardson, C.A., Rendell, H.M., 1995. Luminescence dating of Mojave Desert sands.
306 *Quaternary Science Reviews* 14, 783-789.

307 Durcan, J.A., Duller, G.A.T. 2011. The fast ratio: A rapid measure for testing the dominance of the
308 fast component in the initial OSL signal from quartz *Radiation Measurements* 46, 1065-107.

309 Enzel, Y., Wells, S.G. Lancaster, N. 2003. Late Pleistocene lakes along the Mojave River, southeast
310 California. *Geological Society of America, Special Papers*, 368 pp.61-78.

311 Fuchs, M., Dietze, M., Al-Qudah, K., Lomax, J. 2015. Dating desert pavements – first results from a
312 challenging environmental archive. *Quaternary Geochronology* 30, 342-349.

313 Garcia, A.L., Knott, J.R., Mahan, S.A., Bright, J. 2014. Geochronology and paleoenvironment of pluvial
314 Harper Lake, Mojave Desert, California, USA. *Quaternary Research* 81, 305-317.

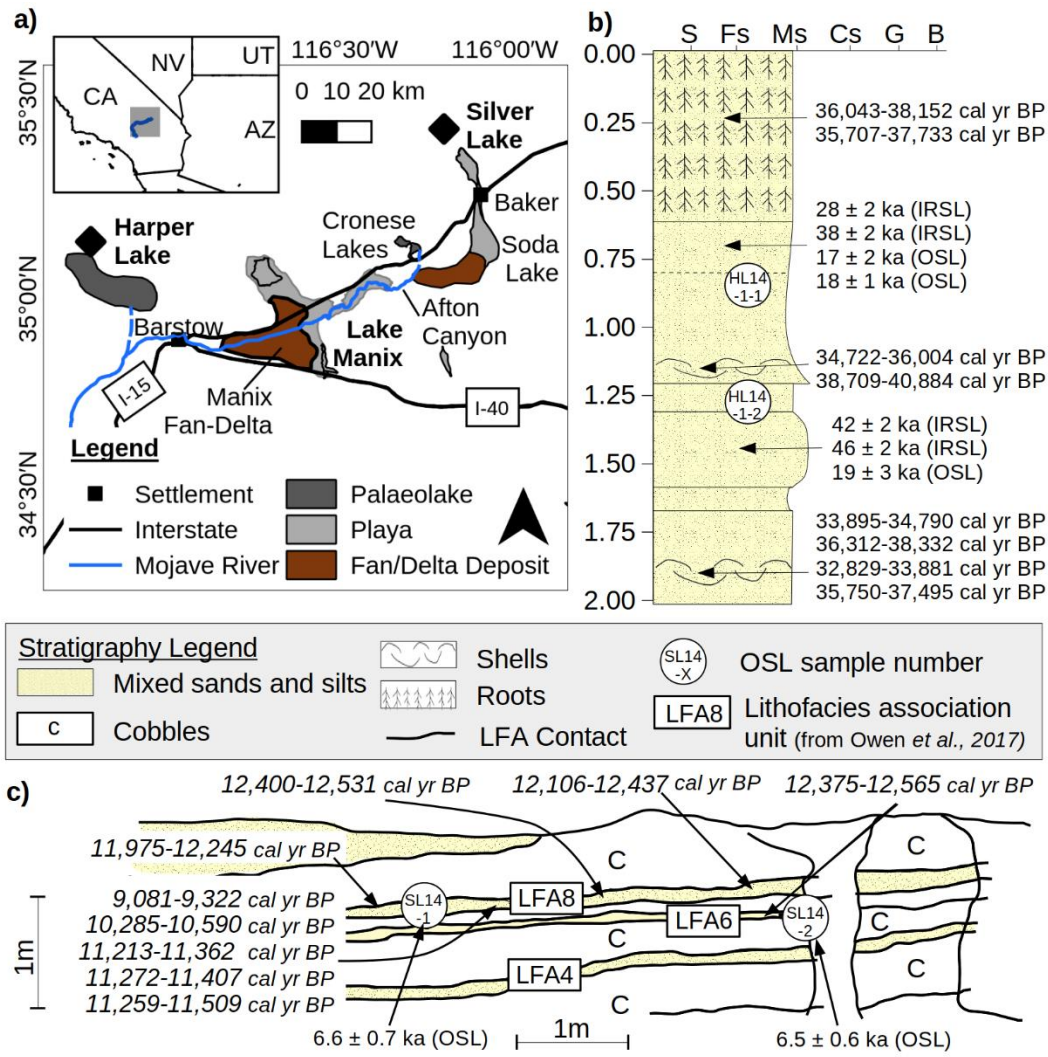
315 Hay, A.S. 2018. The influence of complex topography on aeolian sediment accumulation and
316 preservation: an investigation of morphology and process history. Unpublished PhD thesis,
317 University of Leicester.

318 Huntley, D.J., Lamothe, M. 2001. The ubiquity of anomalous fading in K-feldspars and the
319 measurement and correction for it in optical dating. *Canadian Journal of Earth Science* 38, 1093-
320 1106.

321 Jefferson, G.T. 2003. Stratigraphy and palaeontology of the middle and late Pleistocene Manix
322 Formation, and paleoenvironments of the central Mojave River, southern California. *Geological*
323 *Society of America, Special Papers*, 368, 43-60.

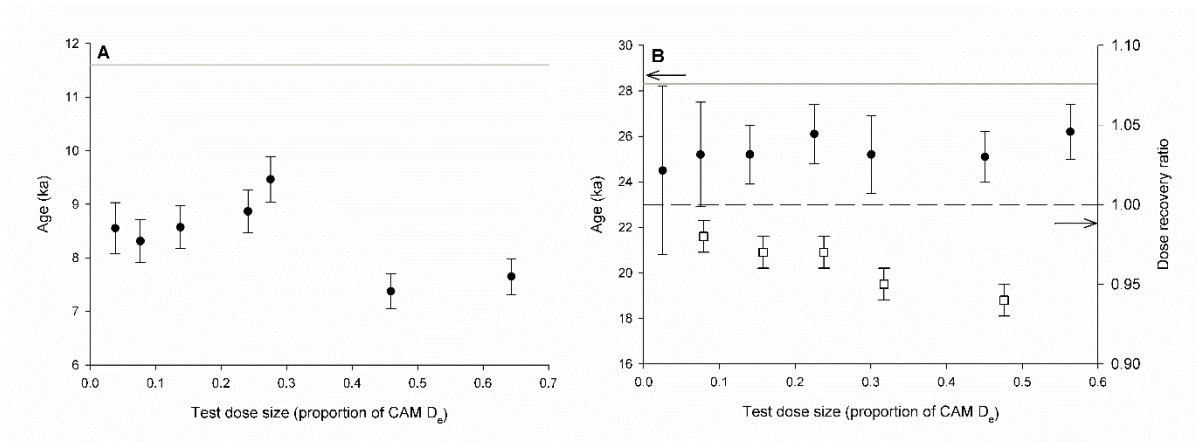
- 324 Kars, R.H., Reimann, T., Wallinga, J. 2014. Are feldspar SAR protocols appropriate for post-IR IRSL
325 dating? *Quaternary Geochronology* 22, 126-136.
- 326 Kreutzer, S., Schmidt, C., Fuchs, M.C., Dietze, M., Fisher, M., Fuchs, M. 2012. Introducing an R
327 package for luminescence dating analysis. *Ancient TL* 30, 1-7.
- 328 Lamothe, M., Barré, M., Huot, S., Ouimet, S. 2012. Natural luminescence and anomalous fading in K-
329 feldspar. *Radiation Measurements* 47, 682-687.
- 330 Lancaster, N., Tchakerian, V.P. 1996. Geomorphology and sediments of sand ramps in the Mojave.
331 *Geomorphology* 17, 151-165.
- 332 Lawson, M.J., Roder, B.J., Stang, D.M., Rhodes, E.J. 2012. OSL and IRSL characteristics of quartz and
333 feldspar from southern California, USA. *Radiation Measurements* 47, 830-836.
- 334 Li, B., Li S-H. 2011. Luminescence dating of K-feldspar from sediments: A protocol without
335 anomalous fading correction. *Quaternary Geochronology* 6, 468-479.
- 336 Li, B., Jacobs, Z., Roberts, R.G. Li, S-H. 2014. Review and assessment of the potential of post-IR IRSL
337 dating methods to circumvent the problem of anomalous fading in feldspar luminescence.
338 *Geochronometria* 41, 178-201.
- 339 Lui, J., Murray, A.S., Sohbaty, R., Jain, M. 2016. The effect of test dose and first IR stimulation
340 temperature on post-IR IRSL measurements of rock slices. *Geochronometria* 43, 179-187.
- 341 McGuire, C., Rhodes, E.J. 2015. Determining fluvial sediment virtual velocity on the Mojave River
342 using K-feldspar IRSL: Initial assessment. *Quaternary International* 362, 124-131.
- 343 Meek, N. 1999. New discoveries about the Late Wisconsinan history of the late Mojave River system.
344 *San Bernadino County Museum Association Quarterly* 46, 113-117.
- 345 Murray, A.S. Wintle, A.G. 2000. Luminescence dating of quartz using an improved single-aliquot
346 regenerative-does protocol. *Radiation measurements* 32, 57-73.
- 347 Ore, H.T., Warren, C.N. 1978. Late Pleistocene-early Holocene geomorphic history of Lake Mojave,
348 California. *Geological Society of America Bulletin* 82, 2553-2562.
- 349 Owen, L.A., Bright, J., Finkel, R.C., Jaiswal, M.K., Kaufman D.S., Mahan, S., Radtke, U., Schneider J.S.,
350 Sharp, W., Singhvi, A.K., Warren, C. 2007. Numerical dating of a Late Quaternary spit-shoreline
351 complex at the northern end of Silver Lake playa, Mojave Desert, California: A comparison of the
352 applicability of radiocarbon, luminescence, terrestrial cosmogenic nuclide, electron spin resonance,
353 U-series and amino acid racemization methods. *Quaternary International* 166, 87-110.
- 354 Reheis, M.C., Bright, J., Lund, S.P., Miller, D.M., Skipp, G., Fleck, R.J. 2012. A half-million-year record
355 of paleoclimate from the Lake Manix Core, Mojave Desert, California. *Palaeogeography,*
356 *Palaeoclimatology, Palaeoecology* 365, 11-37.
- 357 Reheis, M.C., Miller, D.M., McGeehin, J.P., Redwine, J.R., Oviatt, C.G., Bright, J. 2015. Directly dated
358 MIS 3 lake-level record from Lake Manix, Mojave desert, California, USA. *Quaternary Research* 83,
359 187-203.
- 360 Rendell, H.M., Sheffer, N.L. 1996. Luminescence dating of sand ramps in the Eastern Mojave Desert.
361 *Geomorphology* 17, 187-197.

- 362 Rhodes, E.J. 2015. Dating sediments using potassium feldspar single-grain IRSL: initial
363 methodological considerations. *Quaternary International* 362, 14-22.
- 364 Roder, B., Lawson, M., Rhodes, E.J. Dolan, J., McAuliffe, L., McGill, S. 2012. Assessing the potential of
365 luminescence dating for fault slip rate studies on the Garlock fault, Mojave Desert, California, USA.
366 *Quaternary Geochronology* 10, 285-290.
- 367 Smedley, R.K., Duller, G.A.T., Pearce, N.J.G., Roberts, H.M. 2012. Determining the K-content of
368 single-grains of feldspar for luminescence dating. *Radiation Measurements* 47, 790-796.
- 369 Thomsen, K.J., Murray, A.S., Jain, M., Bøtter-Jensen L. 2008. Laboratory fading rates of various
370 luminescence signals from feldspar-rich sediment extracts. *Radiation measurements* 43, 1474-1486.
- 371 Trauerstein, M., Lowick, S.E., Preusser, F., Schlunegger, F. 2014. Small aliquot and single grain IRSL
372 and post-IR IRSL dating of fluvial and alluvial sediments from the Pativilca Valley, Peru. *Quaternary*
373 *Geochronology* 22, 163-174.
- 374 Vermeesch, P. 2009. RadialPlotter: a Java application for fission track, luminescence and other radial
375 plots. *Radiation Measurements* 44, 409-410
- 376 Wells, S.G., Brown, W.J., Enzel, Y., Anderson, R.Y., McFadden, L.D. 2003. Late Quaternary geology
377 and paleohydrology of pluvial Lake Mojave, southern California. *Geological Society of America,*
378 *Special Papers* 358. 79-114.
- 379 Yi, S., Buylaert, J-P., Murray, A.S., Lu, H., Thiel, C., Zeng, L. 2016. A detailed post-IR IRSL dating study
380 of the Niuyangzigou loess site in northeastern China. *Boreas* 45, 644-657.
- 381



383
 384 **Figure 1:** A) Map of the Mojave River catchment, showing the major palaeo-lakes and the present
 385 Mojave River course. B) Site stratigraphy with previously published (calibrated) radiocarbon dates
 386 and luminescence ages for Harper Lake. C) Silver Lake stratigraphy and calibrated radiocarbon age
 387 ranges (modified after Owen et al. 2007).

388
 389
 390

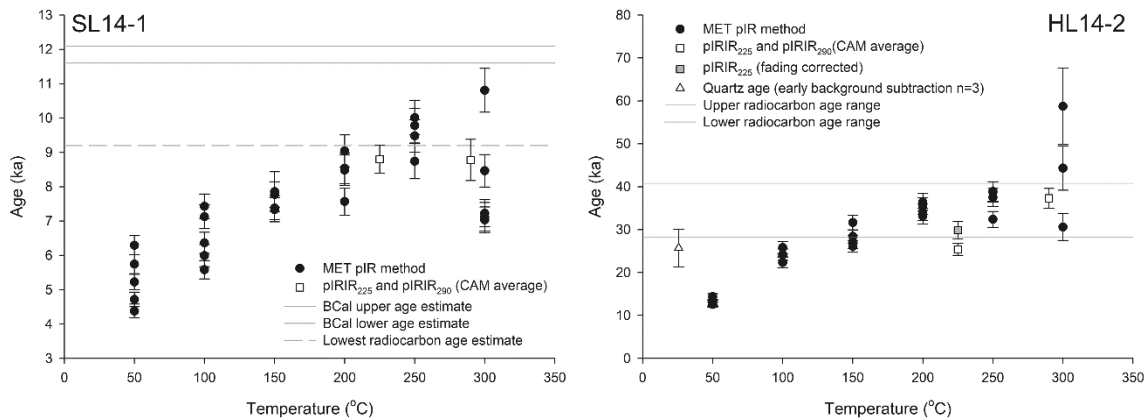


391

392 **Figure 2:** Relationship between test dose size and sample age for (A) Silver Lake SL14-1 and (B)
 393 Harper Lake HL14-1. In A the horizontal line shows the lower 11.6 ka BCal estimate for LFA8 (see
 394 **Table S2**). In B the lowest calibrated (median value) radiocarbon age for HL14-1 is shown with a solid
 395 line; (Meek, 1999), with the natural luminescence signal as filled circles. The HL14-1 dose recovery
 396 results (open squares) are shown on the secondary Y axis and the dashed line marks a dose recovery
 397 ratio of 1. Averages and standard deviations of 3 aliquots are shown.

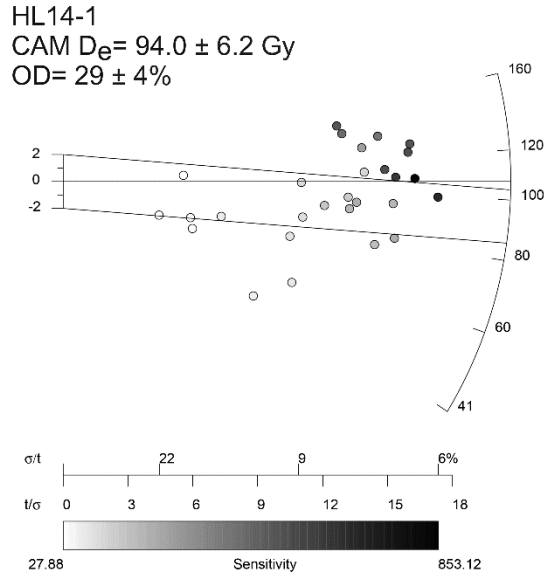
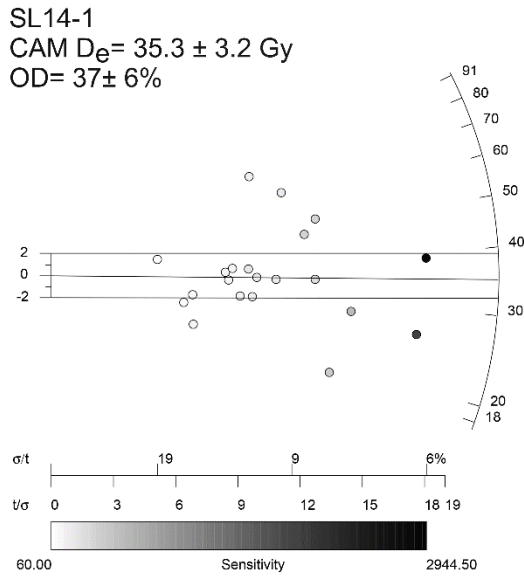
398

399



400

401 **Figure 3:** MET-PIR plateaus and pIRIR₂₂₅ and pIRIR₂₉₀ age estimates for samples SL14-1 and HL14-2.
 402 The BCal age range is shown for SL14-1 (with the median calibrated age for the youngest sample
 403 (AP9) also shown). The range of calibrated radiocarbon ages (median calibrated values in **Table S2**)
 404 are plotted for Harper Lake. Note that the Harper Lake quartz age is from sample HL14-1 (**Table 1**).



405

406

407

408

409

410

411

412

Figure 4: Single grain radial plots (Vermeesch, 2009) for samples SL14-1 and HL14-1. The samples are grey-scaled by sensitivity (first (background subtracted) test dose response in counts $s^{-1} Gy^{-1}$). For Harper Lake the two sigma lines are centred on the CAM estimate for all accepted grains, with the marker line indicating the single aliquot CAM D_e . Similarly, the marker line for SL1-1 is the single aliquot CAM D_e .

413 **Table 1:** Equivalent doses and associated age estimates for the various K-feldspar IRSL methods and the quartz SAR.

Sample	CAM D _e IR 50 (Gy) (n)	Age IR50 (ka)	Age IR50 (ka) Fading correct	CAM D _e pIRIR ₂₂₅ (Gy) (n)	Age pIRIR ₂₂₅ (ka)	Age pIRIR ₂₂₅ (ka) Fading correct	Single grain CAM D _e pIRIR ₂₂₅ (Gy) (n)	Single grain age- pIRIR ₂₂₅ (ka)	CAM D _e pIRIR ₂₉₀ (Gy) (n)	Age pIRIR ₂₉₀ (ka)	CAM D _e Quartz* (Gy) (n)	Age quartz (ka)
SL14-1	25.2 ± 0.95 (20)	6.36 ± 0.30	10.3 ± 0.6	34.9 ± 1.2 (20)	8.8 ± 0.4	10.1 ± 0.5	35.3 ± 3.22 (21)	8.9 ± 0.9	33.1 ± 1.29 (4) [^]	8.4 ± 0.4	16.3 ± 2.0	5.2 ± 0.6
SL14-2	37.4 ± 1.23 (19)	8.26 ± 0.40	12.4 ± 0.8	51.2 ± 1.6 (19)	11.3 ± 0.5	11.9 ± 0.6	nd	nd	nd	nd	nd	nd
HL14-1	54.4 ± 1.91 (22)	13.0 ± 0.70	42.1 ± 20	107 ± 3.5 (22)	25.4 ± 1.4	29.1 ± 1.8	94.0 ± 6.2 (28)	22.4 ± 1.8[#]	140 ± 4.8 (8)	33.4 ± 1.9	85.6 ± 13.8 (3)	25.6 ± 4.3
HL14-2	56.9 ± 2.12 (20)	13.9 ± 0.80	34.6 ± 7.8	104 ± 3.2 (20)	25.4 ± 1.4	29.9 ± 1.8	nd	nd	152 ± 7.0 (8)	37.3 ± 2.3	nd	nd

414

415 [^] No residual subtraction was performed

416 *For Harper Lake the quartz D_e is derived from three acceptable aliquots using early background subtraction

417 # 112.4 ± 6.1 Gy and **26.8 ± 1.9 ka** using the brightest 50% of grains

418 [^]Excluding high outlier aliquot with D_e/age of 42 Gy/ 10.8 ka (**Figure 3**)

419

420

421

422 **Supplementary material – Carr et al.**

423

424 **Table S1:** Details of dose rate determinations

Sample	U (ppm)	Th (ppm)	K (%)	Grain size (μm)	Int. beta dose rate (Gy ka^{-1})	Ext. beta dose rate (Gy ka^{-1})	Gamma dose rate (Gy ka^{-1})	Cosmic dose rate (Gy ka^{-1})	Total dose rate (Gy ka^{-1})
SL14-1	4.08	8.99	1.66	180-250	0.99 ± 0.07	1.54 ± 0.11	1.23 ± 0.48	0.21 ± 0.01	3.96 ± 0.14
SL14-2	2.54	14.2	2.16	180-250	0.99 ± 0.07	1.76 ± 0.13	1.60 ± 0.59	0.19 ± 0.01	4.53 ± 0.16
HL14-1	1.17	4.52	3.02	180-212	0.85 ± 0.06	1.89 ± 0.20	1.24 ± 0.51	0.21 ± 0.01	4.19 ± 0.17
HL14-2	1.97	4.01	2.85	180-212	0.85 ± 0.06	1.86 ± 0.14	1.19 ± 0.48	0.20 ± 0.01	4.10 ± 0.16

425 - Gamma dose rate derived from *in-situ* gamma spectrometry.

426 - Beta dose rates were derived from ICP-MS of sample tube ends, corrected for grain size following
 427 Mejdahl (1979) and Redhead (2002) and water content following Aitken (1985) using element
 428 conversion factors of Guerin et al. (2011). Water contents were $10 \pm 5\%$ and $14.5 \pm 5\%$ following
 429 Owen et al. (2007) and Garcia et al. (2014) (respectively). Measured water contents were 0.6-0.8%
 430 (Harper Lake) and 1.2-1.9% (Silver Lake).

431 - U, Th and K contents derived via ICP-MS with relative uncertainties of 10% (U and Th) and 5% (K).

432 - Internal K and Rb contents were $12.5 \pm 0.5\%$ and 400 ± 100 ppm (Huntley and Baril 1997; Huntley
 433 and Hancock, 2001).

434 - Cosmic dose rates following Prescott and Hutton (1994).

435

436

437 **Table S2:** Published radiocarbon dates from Owen et al. (2007), Garcia et al. (2014) and Meek (1999)
 438 and their calibration using INTCAL13 (Reimer et al., 2013) and CALIB (Stuiver and Reimer, 1993)). The
 439 UCLA and UCR codes for Harper Lake relate to Meek (1999).

Sample	Site	Material	¹⁴ C age (years)	2 sigma calibrated range (cal yr. BP) (probability)	Median age (cal yr. BP)
AP9	Silver Lake LFA8	<i>Anodonta californiensis</i> shell	8240 ± 40	9081-9322 (0.92)	9210
AP10	Silver Lake LFA8	<i>Anodonta californiensis</i> shell	9290 ± 50	10,285-10,590 (0.98)	10,481
AP11	Silver Lake LFA8	<i>Anodonta californiensis</i> shell	9880 ± 40	11,213-11,362 (0.98)	11,271
AP12	Silver Lake LFA8	<i>Anodonta californiensis</i> shell	9790 ± 40	11,272-11,407 (0.76)	11,216
AP3	Silver Lake LFA8	<i>Anodonta californiensis</i> shell	9970 ± 40	11,259-11,509 (0.79)	11,393
AP5	Silver Lake LFA8	<i>Anodonta californiensis</i> shell	10,320 ± 40	11,975-12,245 (0.79)	12,132
AP6	Silver Lake LFA8	<i>Anodonta californiensis</i> shell	10,430 ± 40	12,106-12,437 (0.88)	12,310
AP4	Silver Lake LFA6	<i>Anodonta californiensis</i> shell	10,420 ± 40	12,400-12,531 (1.00)	12,292
AP1	Silver Lake LFA6	<i>Anodonta californiensis</i> shell	10,480 ± 40	12,375-12,565 (0.84)	12,453
ALG-HV-04	Harper Lake Mudflat	<i>Anodonta californiensis</i> shell	32,830 ± 370	36,043-38,152 (1.00)	36,927

ALG-HV-07	Harper Lake Mudflat	<i>Anodonta californiensis</i> shell	32,580 ± 350	35,707-37,733 (1.00)	36,564
ALG-HV-06	Harper Lake Beach	<i>Anodonta californiensis</i> shell	35,230 ± 490	38,709-40,884 (1.00)	39,778
ALG-HV-03	Harper Lake Beach	<i>Anodonta californiensis</i> shell	31,440 ± 310	34,722-36,004 (1.00)	35,328
ALG-HV-05	Harper Lake shoreface	<i>Anodonta californiensis</i> shell	30,340 ± 260	33,895-34,790 (1.00)	34,342
ALG-HV-02	Harper Lake shoreface	<i>Anodonta californiensis</i> shell	33,080 ± 370	36,312-38,332 (1.00)	37,262
ALG-HV-08	Harper Lake shoreface	<i>Anodonta californiensis</i> shell	29,210 ± 240	32,829-33,881 (1.00)	33,412
ALG-HV-09	Harper Lake shoreface	<i>Anodonta californiensis</i> shell	32,540 ± 300	35,750-37,495 (1.00)	36,483
UCR2867	Harper Lake upper shell horizon	<i>Anodonta californiensis</i> shell	25,000± 310	28,375-29,790 (1.00)	29061
UCLA 2627A	Harper Lake upper shell horizon	<i>Anodonta californiensis</i> shell	24,440 ± 2190	24,055-33059 (1.00)	28,576

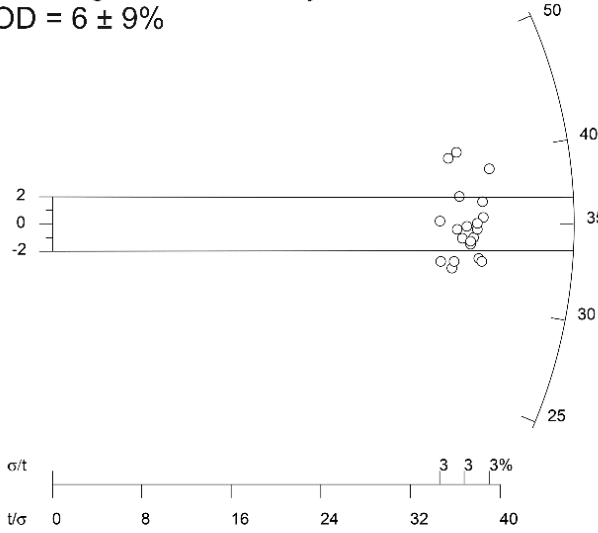
440

441

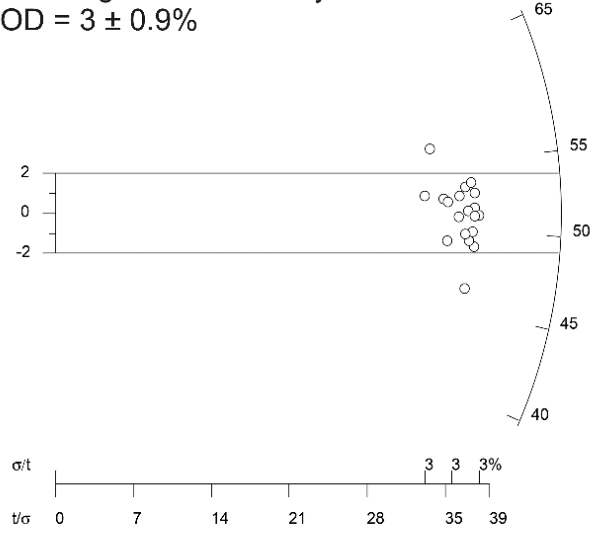
442

443

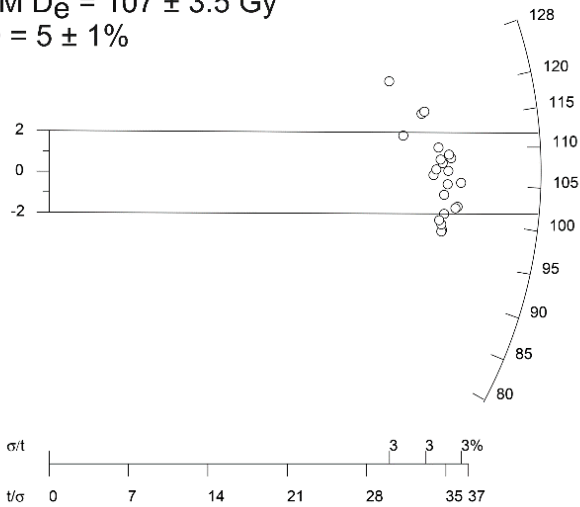
SL14-1
CAM $D_e = 34.9 \pm 1.2$ Gy
OD = $6 \pm 9\%$



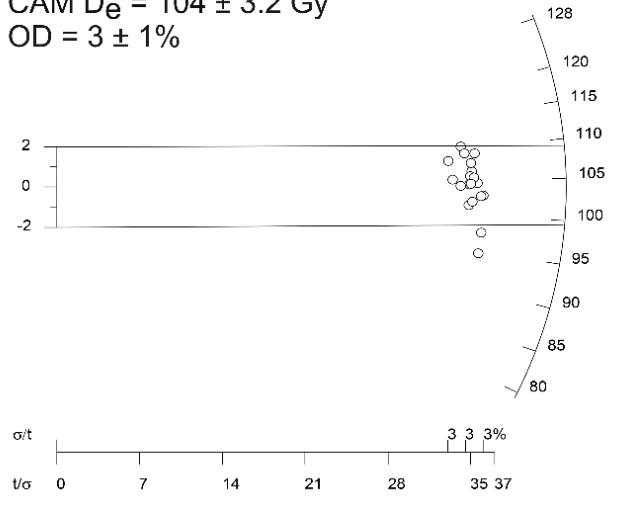
SL14-2
CAM $D_e = 51.2 \pm 1.6$ Gy
OD = $3 \pm 0.9\%$



HL14-1
CAM $D_e = 107 \pm 3.5$ Gy
OD = $5 \pm 1\%$

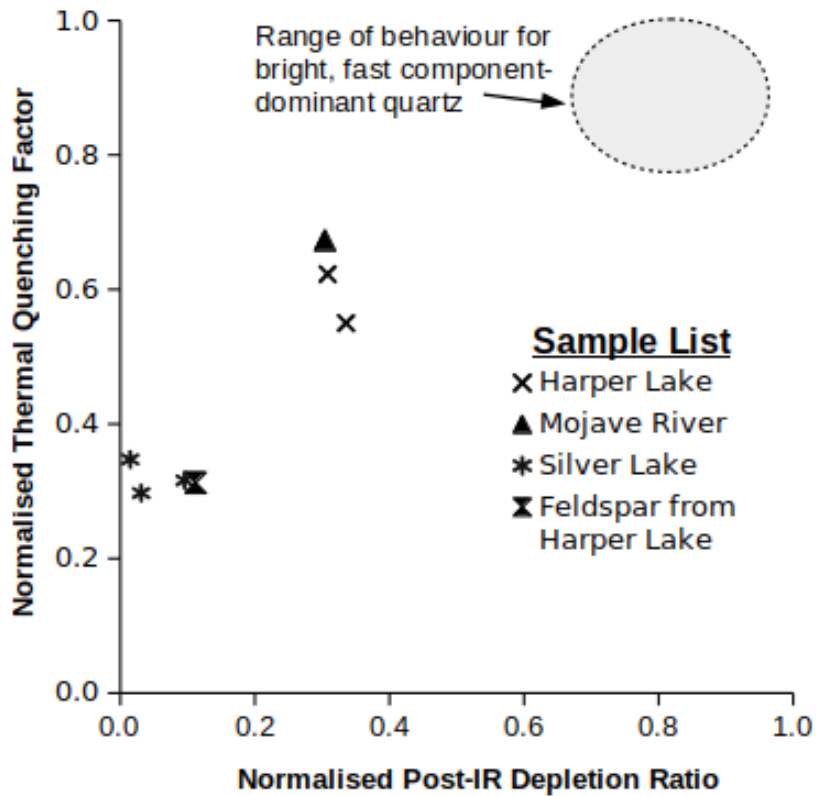


HL14-2
CAM $D_e = 104 \pm 3.2$ Gy
OD = $3 \pm 1\%$



444

445 **Figure S1:** Radial plots for the pIRIR₂₂₅ single aliquot (2 mm) equivalent dose data from Silver and
446 Harper Lake (radial plots were created using the Radial Plotter software of Vermeesch (2009)).



447

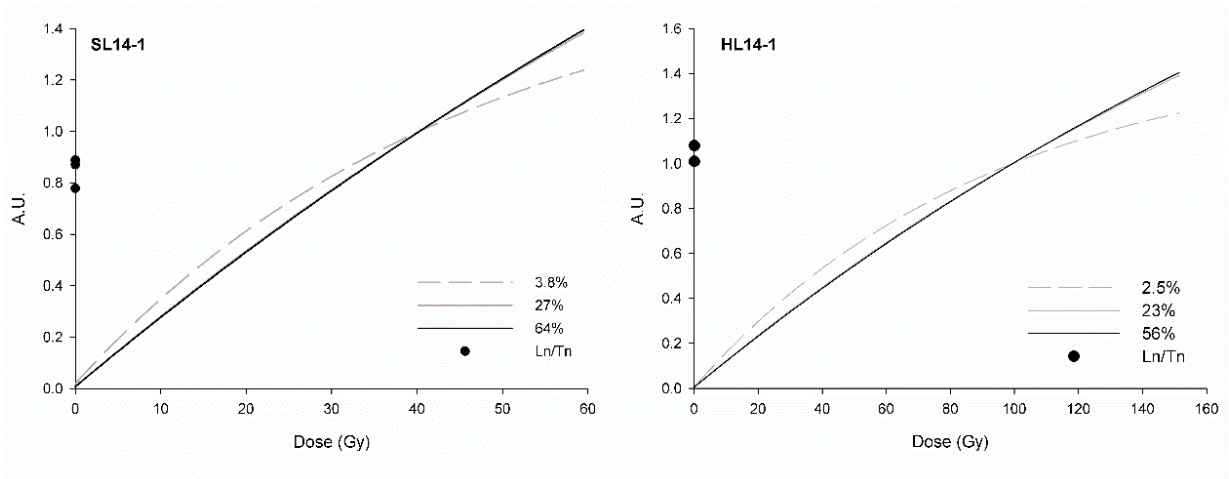
448 **Figure S2:** Quartz IR-bleaching and thermal quenching contamination test results (following Lawson
 449 et al., 2012) for the Silver Lake and Harper Lake coarse-grained quartz extracts. Also shown is a
 450 sample from the modern Mojave River bed (filled triangle) to provide a comparative indication of
 451 the behaviour of quartz in the wider Mojave catchment. The grey circle indicates the typical range
 452 for quartz extracts with a bright, fast component-dominated quartz OSL signal (samples from
 453 numerous locations around the world as analysed in our laboratory).

454

455

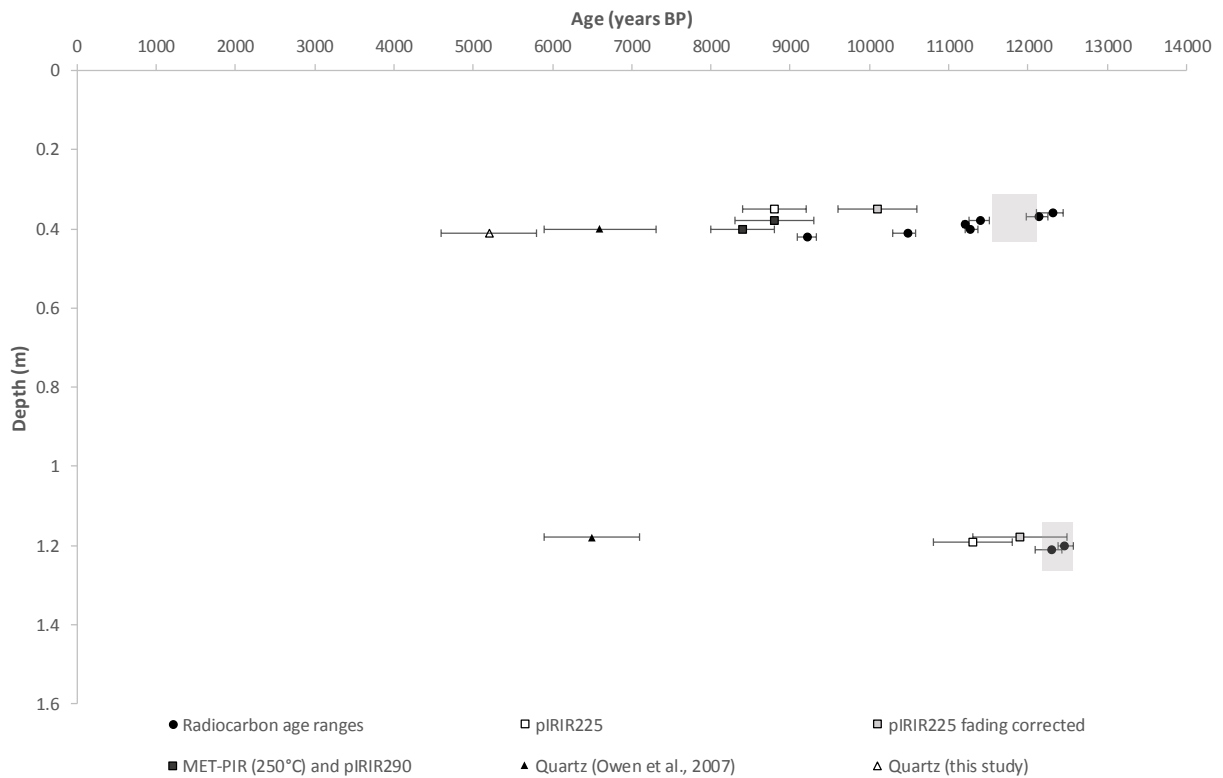
456

457

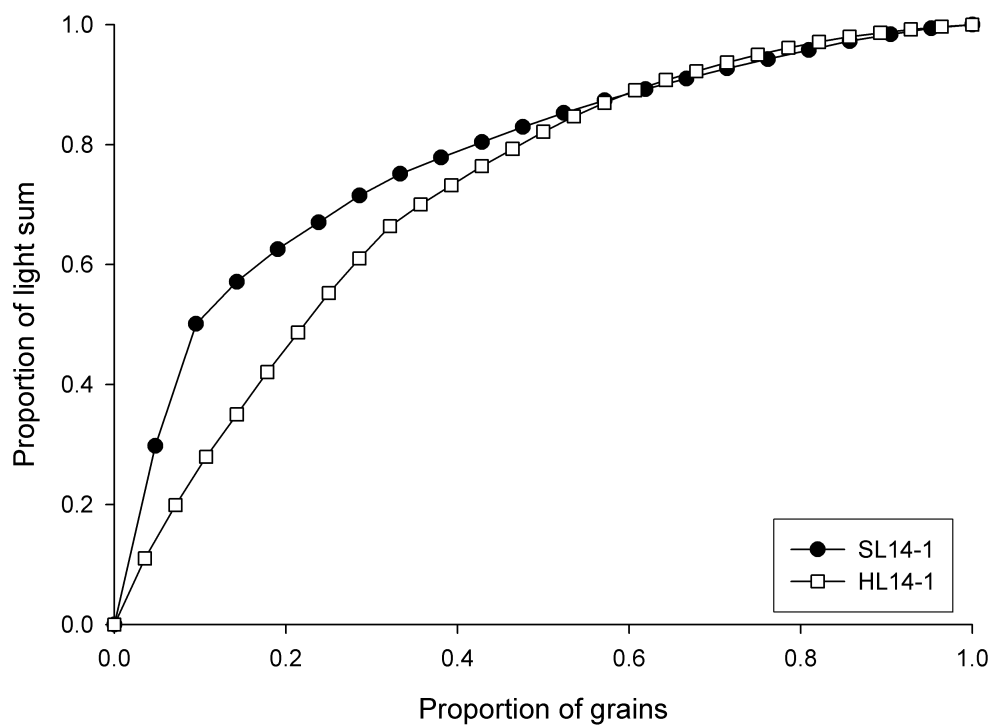


458

459 **Figure S3:** The effect of test dose size on dose response curve form, as derived from pIRIR₂₂₅ natural
 460 D_e measurement sequences. The data are averages of three aliquots and have been normalised to
 461 the 40 Gy (SL14-1) and 90 Gy (HL14-1) regeneration doses. The lower Ln/Tn for the highest test dose
 462 at Silver Lake is indicated. At Harper Lake the lower Ln/Tn value relates to the lowest (2.5%) test
 463 dose.
 464



465
 466 **Figure S4:** Compared age estimates for the Silver Lake Silver Quarry site LFA 8 and LFA6 as obtained
 467 in this study and by Owen et al. (2007). The grey boxes represent the BCal age ranges (*ibid*).
 468

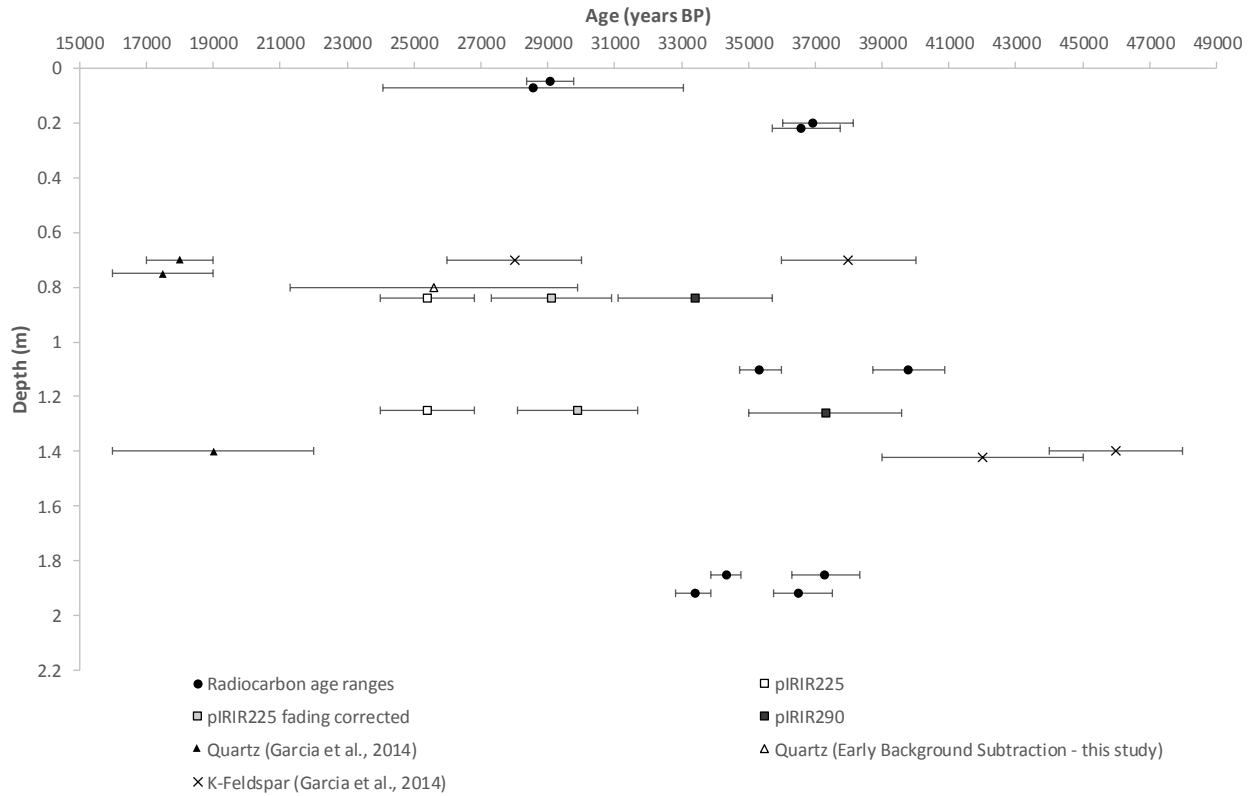


470

471 **Figure S5:** pIRIR₂₂₅ single grain brightness distributions for samples SL14-1 and HL14-1.

472

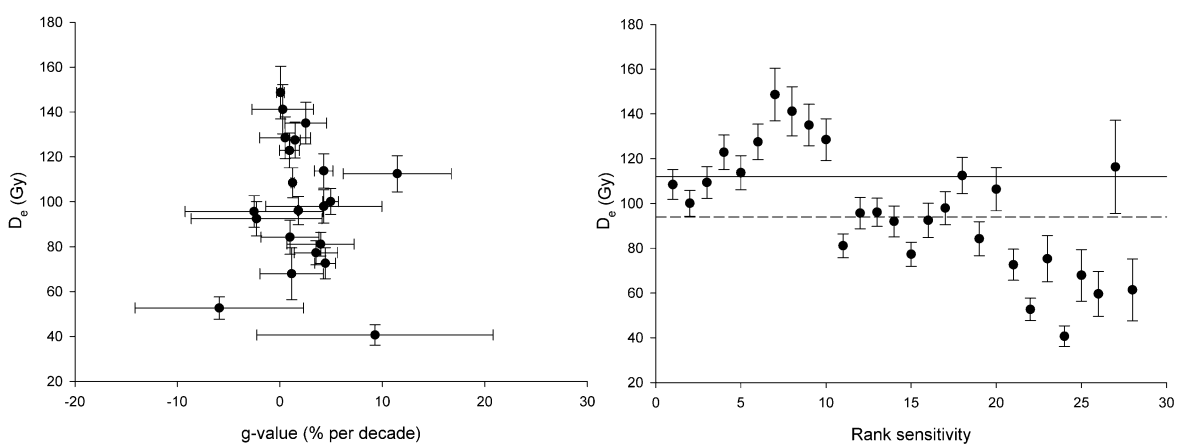
473



474

475 **Figure S6:** Compared age estimates for the Harper Lake Mountain View Hill site, plotted by depth,
 476 including the post-IR IRSL and quartz OSL ages from this study, the MAAD IRSL, quartz OSL ages and
 477 calibrated radiocarbon ages from Garcia et al. (2014), and the calibrated radiocarbon ages reported
 478 in Meek (1999). The two upper-most radiocarbon samples are from Meek (1999) and have been
 479 assigned arbitrary depths for the purposes of illustration.

480



481

482 **Figure S7:** Left: The relationship between individual grain pIRIR₂₂₅ fading rates and single grain D_e
 483 for sample HL14-1. Right: Single grain equivalent doses plotted by rank sensitivity (following Rhodes,
 484 2015) for HL14-1. The dashed line is the CAM D_e for all grains and the solid line the CAM D_e for the
 485 brightest 50% of grains (112 ± 6 Gy).

486

487 **References**

- 488 Aitken, M.J 1985. Thermoluminescence Dating. Academic Press, 370p
- 489 Garcia, A.L., Knott, J.R., Mahan, S.A., Bright, J. 2014. Geochronology and paleoenvironment of pluvial
490 Harper Lake, Mojave Desert, California, USA. Quaternary Research 81, 305-317.
- 491 Guérin, G., Mercier, N., Adamiec, G. 2011. Dose-rate conversion factors: update. Ancient TL 29, 5-8.
- 492 Huntley, D.J., Baril D.J. 1997. The K content of the K-feldspars being measured in optical dating or in
493 thermoluminescence dating. Ancient TL 15, 11–13
- 494 Huntley, D.J., Hancock, R.G.V. 2001. The Rb contents of the K-feldspars being measured in optical
495 dating. Ancient TL 19, 43–46
- 496 Lawson, M.J., Roder, B.J., Stang, D.M., Rhodes, E.J. 2012. OSL and IRSL characteristics of quartz and
497 feldspar from southern California, USA. Radiation Measurements 47, 830-836.
- 498 Meek, N. 1999. New discoveries about the Late Wisconsinan history of the late Mojave River system.
499 San Bernadino County Museum Association Quarterly 46, 113-117.
- 500 Mejdahl, V. 1979 Thermoluminescence dating: beta-dose attenuation in quartz grains.
501 Archaeometry 21, 61-72.
- 502 Owen, L.A., Bright, J., Finkel, R.C., Jaiswal, M.K., Kaufman D.S., Mahan, S., Radtke, U., Schneider J.S.,
503 Sharp, W., Singhvi, A.K., Warren, C. 2007. Numerical dating of a Late Quaternary spit-shoreline
504 complex at the northern end of Silver Lake playa, Mojave Desert, California: A comparison of the
505 applicability of radiocarbon, luminescence, terrestrial cosmogenic nuclide, electron spin resonance,
506 U-series and amino acid racemization methods. Quaternary International 166, 87-110.
- 507 Prescott, J.R., Hutton, J.T. 1994. Cosmic ray contributions to dose rates for luminescence and ESR
508 dating: Large depths and long-term time variations. Radiation Measurements 23, 497-500.
- 509 Readhead, M.L., 2002. Absorbed dose fraction for ⁸⁷Rb beta particles. Ancient TL 20, 25-29.
- 510 Reimer, P.J., Bard, E., Bayliss, A., Beck, J.W., Blackwell, P.G., Ramsey, C.B., Buck, C.E., Cheng, H.,
511 Edwards, R.L., Friedrich, M. Grootes, P.M. 2013. IntCal13 and Marine13 radiocarbon age calibration
512 curves 0–50,000 years cal BP. Radiocarbon 55, 1869-1887.
- 513 Rhodes, E.J. 2015. Dating sediments using potassium feldspar single-grain IRSL: initial
514 methodological considerations. Quaternary International 362, 14-22.
- 515 Stuiver, M. Reimer, P.J., 1993. Extended ¹⁴C data base and revised CALIB 3.0 ¹⁴C age calibration
516 program. Radiocarbon 35, 215-230.
- 517 Vermeesch, P. 2009. RadialPlotter: a Java application for fission track, luminescence and other radial
518 plots. Radiation Measurements 44, 409-410

519